Nano-Mechanical and Tribological Characteristics of Ultra-Thin Amorphous Carbon Film Investigated by AFM

Koo-Hyun Chung, Jae-Won Lee, Dae-Eun Kim*
School of Mechanical Engineering, Yonsei University, Seoul 120-749, Korea

The mechanical as well as tribological characteristics of coating films as thin as a few nm become more crucial as applications in micro-systems grow. Especially, the amorphous carbon film has a potential to be used as a protective layer for micro-systems. In this work, quantitative evaluation of nano-indentation, scratching, and wear tests were performed on the 7nm thick amorphous carbon film using an Atomic Force Microscope (AFM). It was shown that AFM-based nano-indentation using a diamond coated tip can be feasibly utilized for mechanical characterization of ultra-thin films. Also, it was found that the critical load where the failure of the carbon film occurred was about 18μN by the ramp load scratch test. Finally, the wear experimental results showed that the quantitative wear rate of the carbon film ranged $10^{-9}\sim10^{-8}$ mm^3/N cycle. These experimental methods can be effectively utilized for a better understanding the mechanical and tribological characteristics at the nano-scale.

Key Words : Atomic Force Microscope (AFM), Diamond Coated Tip, Nano-Indentation, Nano-Wear Rate, Scratch Test

1. Introduction

Amorphous carbon coating films have been widely utilized for precision mechanical components due to their high surface hardness, low frictional characteristics, and chemical inertness (Liu et al., 1996, Robertson, 1992, Staedler and Schiffman, 2001). For example, hard amorphous carbon film has been widely employed as a protective layer of the slider as well as of the disk in a hard disk drive, and consequently, excellent durability has been realized. It is well known that the chemical structure and property of the amorphous carbon film is largely dependent on the deposition process and conditions. Also, it has been reported that the high hardness can be obtained by stabilizing the sp^3 bondings and increasing the sp^3/sp^2 ratio based on the effect of hydrogen (Angus and Hayman, 1988). The typical hardness of the amorphous carbon film ranges in the order of tens of GPa and the ultra-low friction coefficient of below 0.01 has been achieved (Bhushan, 1999a, Erdemir et al., 1997). Since commercialization of the micro-mechanical components has been hampered by durability limitations, amorphous carbon coating films have a great potential to be used as the protective coating layer for micro-systems based on these superior tribological characteristics (Bhushan, 1998).

The importance of the ultra-thin film became more crucial with the development of micro-systems such as Micro-Electro-Mechanical-Systems (MEMS). Particularly, for accomplishing the areal density of over 100 $Gbit/in^2$, it has been suggested that the thickness of the carbon film should be decreased to as thin as a few nm (Menon, 2000). In order to evaluate the mechanical properties of the ultra-thin film, such as elastic modulus, surface hardness, and fracture toughness, the nano-indentation experimental methods have been utilized. By using the load-displacem-

* Corresponding Author,
E-mail : kimde@yonsei.ac.kr
TEL : +82-2-2123-2822; **FAX** : +82-2-312-2159
School of Mechanical Engineering, Yonsei University, Seoul 120-749, Korea (Manuscript **Received** March 18, 2004; **Revised** June 29, 2004)

ent curve obtained during the nano-indentation process, the hardness and elastic modulus can be measured (Oliver and Pharr, 1992). The most widely used tip is the Berkovich indentor which has a three-sided pyramidal shaped diamond tip. The typical load of the commercial nano-indentor ranges between 0.2 to 10mN and the available indentation depth is in the range of a few tens of nm (Bhushan, 1999b). Using an AFM equipped with the nano-indentation capabilities, the indentation mark can be observed more precisely (Martinez et al., 2001). By using this system, it became possible to gain a better understanding of the material behavior by nano-indentation. Furthermore, to obtain the mechanical property of the coating films of below 100nm in thickness, AFM-based nano-indentation has been developed. For the AFM-based nano-indentation, specially prepared diamond tip has been mounted on the stiff cantilever and the indentation depths as small as a few nm were obtained by the load of about 60~100μN (Bhushan and Koinkar, 1994). In addition, it has been reported that the nano-mechanical properties of ductile materials, such as polymer and gold were characterized by the indentation using a silicon AFM tip (Krache and Damaschke, 2000, Lemoine and Laughlin, 1999). However, more experimental as well as theoretical analyses are needed, to understand the mechanical characteristics of ultra-thin coating films as thin as a few nm.

For the tribological characterization of ultra-thin films, the scratch test has been typically adopted (Huang et al., 2002, Sundararajan and Bhushan, 1998, Zhao et al., 2002). Ramp-load scratch test has been effectively utilized for evaluation of the adhesion of coating films as well as scratch resistance of various materials. Using the scratch test, the critical load for the separation of the coating film from the substrate can be obtained, and, the failure model of the coating films can be characterized (Bull, 1997, Valli et al., 1985). Since tribological as well as the material behavior of the thin film during the scratch test can be understood by monitoring the friction force (Bellido-Gonzalez et al., 1995), the scratch tester with the friction force monitoring option has been commercialized. Conventionally, the scratch test was performed by using the hard diamond stylus with a tip radius of 1~500μm and the scratch depth was in the μm-scale. Therefore, the mechanical property measurement and tribological characterization for a few μm thick films could be performed. With the emergence of the nano-indentor, the Berkovich tip which has a radius of below 100nm has been widely used for scratch tests as well. Since the load range was decreased to about mN, the thin film characterization in the nm scale has been possible. In addition, by using an AFM configuration, the scratch test load in the μN~nN range has been realized, and this has allowed the film thickness in the nm regime to be analyzed by the scratch test (Chung and Kim, 2003, Sundararajan and Bhushan, 1998).

The mechanical and tribological behaviors of the coated film as thin as a few nm are not clearly understood though numerous researches have been performed. This is due to the fact that quantitative as well as qualitative evaluation of ultra-thin film at the nm level is not straightforward as nano-scale interactions between materials and mechanics are not fully understood. Moreover, since the mechanical as well as tribological characteristics of carbon coated films are largely dependent on the deposition process and conditions, data can not be directly compared. The motivation of this work was to gain a better understanding of the mechanical as well as tribological characteristics of the ultra-thin film at the nano level. Particularly, by using the AFM-based indentation method, the mechanical property of the 7nm thick amorphous carbon film was characterized. Failure of the coating film and quantitative assessment of wear at extremely low loads was also sought by the scratch test.

2. Experimental Details

In this work, the AFM-based indentation, scratch, and wear tests were performed to quantitatively assess the nano-mechanical and the tribological characteristics of amorphous carbon films. For these experiments, an AFM from Park

Scientific Instrument (AutoProbe M5) was used. As for AFM probe tips, polycrystalline diamond coated AFM tips were utilized for indentation, scratch, and wear test and Si tips were used for measurement of the indentation mark and wear track after the experiments. The widths, lengths, and thicknesses of the cantilevers were obtained from the Scanning Electron Microscope (SEM) micrographs and the stiffness of each tip was calculated. The vertical stiffness of the cantilever where the polycrystalline diamond tip was located was about 46N/m and that of the Si tip was about 0.1N/m. The nominal tip radius of the polycrystalline diamond coated tip and Si tip was about 100~200nm and 10nm, respectively. As for the coated specimens, the ultra-thin amorphous carbon films coated on Si (100) substrates by DC magnetron sputtering method were used. The thickness was measured by using ellipsometry and the result showed that the value was about 7.3nm.

Nano-indentation tests using the polycrystalline diamond coated tip were conducted under 1, 2, 5, 7, and 10μN of load, and each indentation mark was observed by the AFM. The wear tests between the tip and the specimen were performed. The normal load used for the wear tests ranged between 0.5 and 4μN. The reciprocating speed was 1μm/s and the distance was 2μm. In addition, failure characteristics of the ultra-thin coated film was evaluated by employing the ramp load scratch test where the normal load was increased from 0 to about 20μN with the simultaneous movement of the specimen at 0.2μm/s speed was performed. The total scratch distance was about 1.7μm. During this experiment, the lateral force was monitored. Also, the lateral force was calibrated using a tipless cantilever as suggested by a previous research (Bogdanovic, 2000). All the experiments were performed in Class 100 environment at the room temperature and the relative humidity was about 30%.

For the quantitative assessment of the wear characteristics of the carbon film, the wear and the scratch tracks were observed by using the Si AFM tip. Also, before and after the experiment, the damage of polycrystalline diamond tips was examined by an SEM. In addition, since the shape of the polycrystalline diamond tip was quite random, the shape of the tip end was measured by the Si AFM tip in the contact mode. The measurement load was minimized to be about a few nN to eliminate the damage of the polycrystalline diamond tip due to the AFM imaging. By doing so, more exact radius and shape of the tip could be obtained, and therefore, this method was effectively utilized for the contact analysis in this work. The indentation mark, wear track, and ramp load scratch track, were measured by the AFM using the Si tip under a few nN to minimize the surface damage during the measurement.

3. Nano-indentation Test

Nano-indentation was performed on the ultra-thin carbon film by using the polycrystalline diamond tip mounted on the AFM cantilever. The 3D and 2D AFM images of the polycrystalline diamond coated tip used in this experiment are given in Fig. 1. The 2D images at the highest position of the tip were extracted from the 3D image. The AFM tip was scanned in the area of $1\times1\mu m^2$ scan area as shown in Fig. 1 (a) and a more magnified AFM image of the end of the tip was obtained in the $0.3\times0.3\mu m^2$ scan area. The shape of the diamond tip was roughly conical and the tip radius was about 120nm which can be seen in Figs. 1 (a) and (b). In order to find the exact shape of the tip and monitor the tip wear during the test, it was helpful to observe the tip shape by an AFM as mentioned in previous studies (Khurshudov and Kato, 1995, Petzold et al., 1995).

The indentations were performed under 0.9~20 μN load by using the polycrystalline coated diamond tip shown in Fig. 1. When the indentation load was over 10μN, it seemed that the tip scratched the carbon surface in the axial direction of the cantilever. Since the stiffness of the cantilever was 46N/m, the vertical deflection was calculated to be about 435nm for the 20μN normal load. Considering the degree of this vertical deflection and the cantilever mounting angle of about 10°, the axial deflection of the cantilever was expected to be about a few nm in the case of a few μN

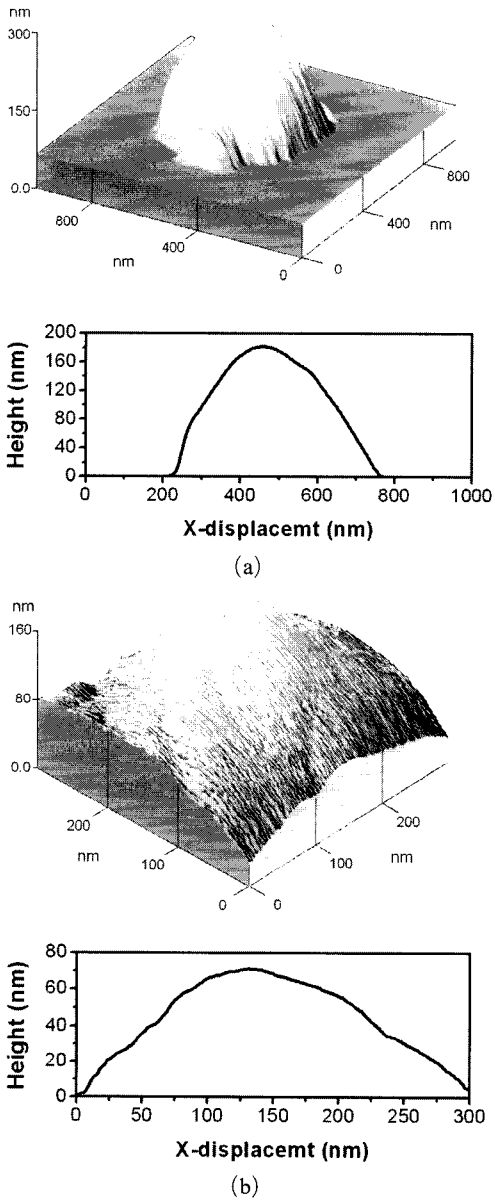

Fig. 1 3D and 2D AFM profiles of the highest position of the polycrystalline diamond coated tip before experiment : scanned in the area of (a) $1.0\times1.0\mu m^2$ and (b) $0.3\times0.3\mu m^2$

indentation load. However, if the normal load was in the range of the $10\sim20\mu N$, the deflection of the cantilever was expected to be in the order of tens of nm. Since the diameter of the indentation area was over $20\sim50$nm, the experimental data from indentation load of $10\mu N$ or less were used for evaluation.

As shown in Fig. 2, the indentation mark clearly formed under $0.9\mu N$ peak indentation load on the 7nm thin amorphous carbon film. The AFM scan area was $0.2\times0.2\mu m^2$. The 2D profile of the indentation mark at the deepest position and the tip profile are shown in Fig. 2 (b). It could be seen that both profiles were matching quite well. The depth of the indentation mark was slightly lower than the height of tip profile when the two profiles were positioned at the same width. The maximum depth was about 1.4nm.

Based on the Hertzian contact theory, the contact pressure was calculated. Since the mechanical property of the carbon film used in this work was unknown, the nano-indentation was performed on the 300nm thick carbon film which was deposited by the same method using the commercial nano-indentor with about 40nm indentation depth. The elastic modulus and the hardness were obtained to be about 130 GPa and 12 GPa, respectively. As for the polycrystalline diamond, the value of 500 GPa was used as the elastic modulus. By using these values, the contact radius and mean pressure were calculated to be about 10nm and 3.4 GPa. This value was about 25% of the hardness of the amorphous carbon film measured by a commercial nano-indentor. It was suspected that the higher pressure would be applied at the asperity on the carbon surface during indentation. Also, nonlinearity in the force-distance curve due to the plastic behavior of the indented material was observed during the nano-indentation process. Therefore, it can be deduced that the plastic deformation of the asperities under the tip occurred as observed in Fig. 2.

By using the AFM-based indentation method, it was expected that the hardness value can be roughly estimated by using the following equation :

$$H=\frac{P_{max}}{A} \tag{1}$$

where P_{max} is the peak indentation load and the A is the projected area of the indentation mark. From the AFM measurement shown in Fig. 2, the projected area of the indentation mark was measured to about $0.0006\mu m^2$, and therefore, the hard-

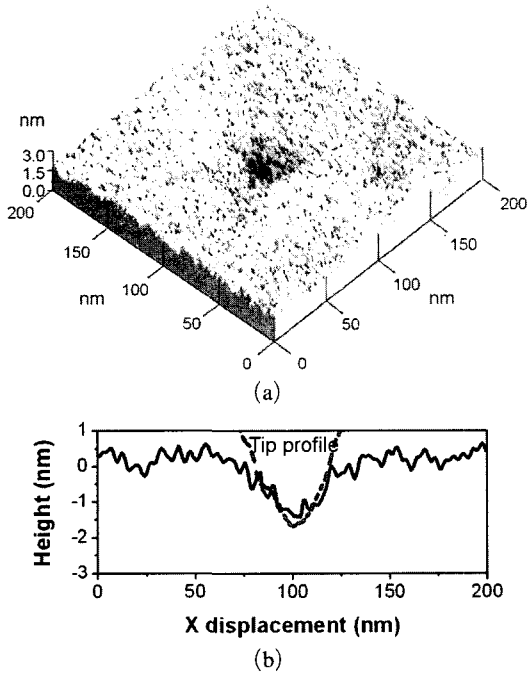

Fig. 2 (a) 3D AFM image and (b) 2D profile at the deepest indentation mark : 0.9μN peak indentation load

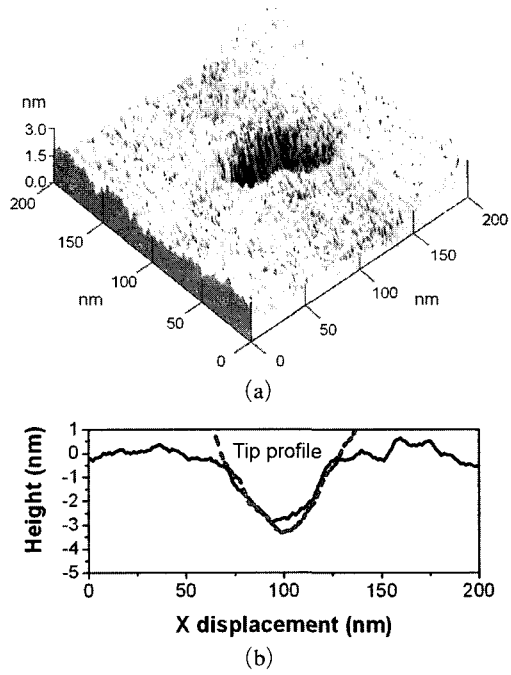

Fig. 3 (a) 3D AFM image and (b) 2D profile at the deepest indentation mark : 9.5μN peak indentation load

ness was estimated to be about 1.5 GPa. This value was significantly lower than the value measured by the commercial nano-indentor (12 GPa). Since the asperities on the carbon film supported the tip at the initial stage of the indentation, a certain portion of the indented depth was affected by the asperity deformation. From Fig. 2 (a), the micro-asperities at the roughness level could be observed on the indented area. In addition, since the density of the film may decrease as the thickness decreases the relatively low density of the amorphous carbon film used in this experiment may have been responsible for the low hardness value. Therefore, the hardness was significantly smaller than the expected value.

The 3D AFM image of the indentation mark under the 9.5μN peak load and the 2D profile at the deepest position are given in Fig. 3. As expected, the indentation mark was significantly larger compared to the 0.9nN load case shown in Fig. 2 (a). However, it should be noted that the effect of axial deflection of the cantilever during the indentation process could not be entirely avoided. As a consequence, the maximum indentation depth was about 3nm and this value was quite lower than the indented depth of the tip. It was attributed to the elastic recovery of the surface after the indentation. In this case, the mean Hertzian contact pressure was about 7.5 GPa. The projected indentation area was about 0.0012μm^2, and the hardness was calculated to be about 8 GPa, which was significantly larger than the calculated value from the 0.9μN indentation case. Since indentation depth was half of the film thickness, the effect of the substrate on reduction of the hardness may not be ignored due the defects at the interface or deformation of the substrate itself. However, it can be concluded that the AFM-based indentation by using the diamond coated tip can be effectively utilized for surface hardness approximation of the coating film as thin as a few nm in the case of very smooth surfaces.

4. Ramp Load Scratch Test

The scratch test at micro/nano-scale has been

widely used for analysis of the scratch or wear resistance and the failure mode of the coated films revealing the adhesion (Bhushan, 1999a, Bull, 1997). Before the wear test, the ramp load scratch test was performed by using the polycrystalline diamond coated tip on the amorphous carbon film as thin as 7nm by using an AFM. The scratch area was measured by the AFM after the test.

The normal load was increased from 0 to about 40μN during 1.7μm scratching distance. The 3D AFM images of the scratched area are given in Figs. 4 and 5. In order to observe the mark by the ramp load scratching more precisely, the initial and final parts of the track were measured individually. Also, the normal and friction force variations during the test are shown in Fig. 6. Due to coupling effect of the cantilever deflection during the ramp load scratching, the scratch track was not straight after the scratch length of 0.8μm. However, it is quite sufficient to evaluate the characteristics of the coated film failure by using this method. The AFM measurement results of the initial 0.8μm and the final 0.9μm scratch marks were given in Figs. 4 and 5. It was shown that the first burr was formed at the side of the scratch test after about 250nm sliding, which corresponded 5μN normal load. This could be found from the 2D profile of cross-section A-A′ and the burr height was about 3nm as shown in Fig. 4 (b). These burrs were expected to be formed by the plastic flow of the coated film itself, since the coated film was not entirely removed and the amount the burrs was comparable to that of the removed carbon at the scratched area. Also, in Fig. 4 (b), the initial wear track formation which could be observed by the AFM was indicated by 'a'. The cross-section of B-B′, which corresponded to 'b' position in Fig. 4 (b) was given in Fig. 4 (c). After 650nm sliding distance which corresponded to 18μN normal load, the wear track depth increased to about 7nm which was the coating thickness of the amorphous carbon film. Therefore, it could be concluded that the critical load where the coated film failure occurred was about 18μN. It was clearly seen that the coating film was entirely removed and the Si substrate was exposed beyond this load. After the

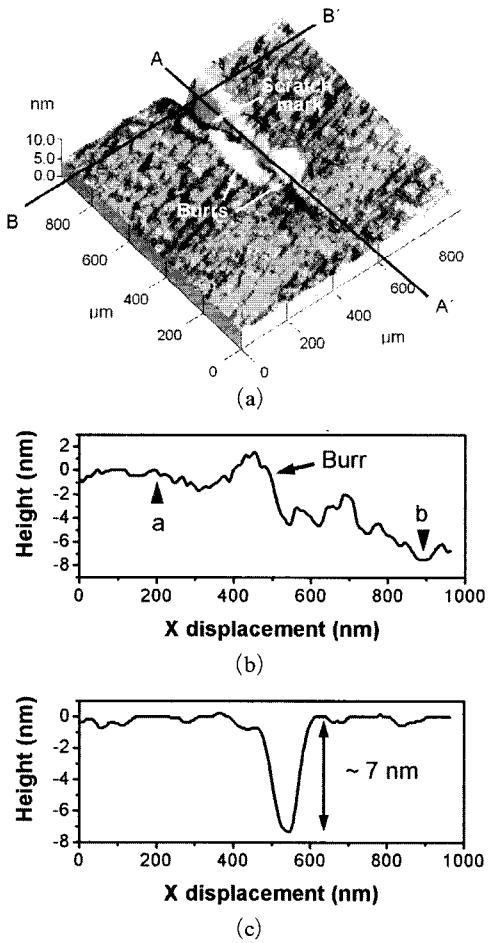

Fig. 4 AFM image of initial 0.8μm scratch mark : (a) 3D AFM image, (b) 2D profile of A-A′ cross-section, and (c) 2D profile of B-B′ cross-section

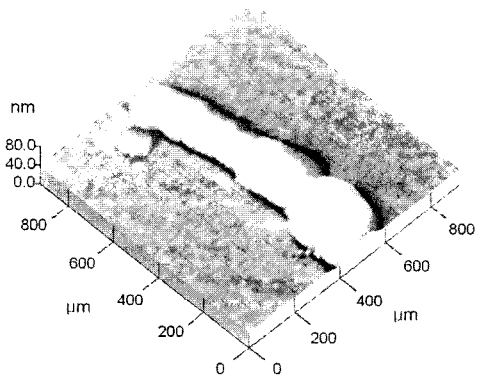

Fig. 5 3D AFM image of final 0.9μm scratch mark

coated film failure, a large amount of the burr was generated as can be seen in Fig. 5. Since the amount of the burrs was significantly larger than that of the scratch mark, it was believed that buckling or delamination of the coated film occurred. These phenomena can be well correlated with the friction force profile shown in Fig. 6. At the initial stage of the ramp load scratch where the plastic deformation of the film occurred, the friction force increased quite linearly. However, with the burr formation, the friction force began to oscillate significantly. After the coating film failure occurred at about 18μN normal load, the friction force increased again with some oscillation.

In summary, the critical load of the ultra-thin film could be found by the ramp load scratch test using an AFM. The critical load of the 7nm thick amorphous carbon film used in this experiment was about 18μN. This value was quite low compared with the value reported in the previous research (Bhushan, 1999a). This discrepancy is probably due to the difference in the mechanical properties of the coated film and the shape of the scratch tip, which can significantly affect the contact pressure during the test. Also, it was shown that the characteristics of the failure could be assessed by observing the scratch track and monitoring the friction force. It should be noted that the critical load of the ultra-thin film obtained from this experimental method can be effectively utilized for optimization of scribing conditions for the micro/nano-machining such as Mechano-Chemical Scanning Probe Lithography (Sung and Kim, 2003).

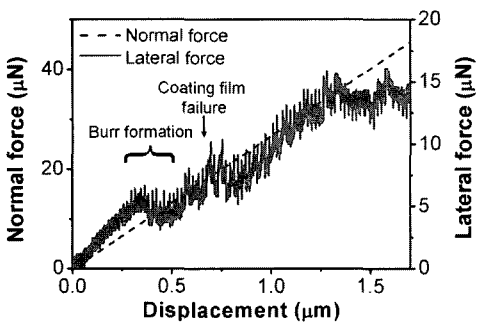

Fig. 6 Normal force and lateral friction variations during ramp load scratch test

5. Nano-wear Test

Following the scratch tests, experiments were performed to assess the nano-wear characteristics of the carbon films based on the ramp load scratch experimental results. The applied normal loads for the wear test were determined to be 0.5, 1, 2, and 4μN. The maximum load of 4μN was chosen so that the coated film will not fail. The reciprocating cycles for the wear tests were 10, 20, 30, 50, 70, and 100 cycles. After the wear test, the wear track was observed by the AFM.

Figure 7 (a) shows the AFM image of wear track of the carbon film after 10, 20, and 30 cycles of sliding under 0.5μN normal load. It could be seen that the carbon film was slightly scribed and no significant burr was formed. However, as shown in Fig. 7 (b), the wear occurred seriously and a lot of wear debris was generated after 70 and 100 cycles of sliding under 4μN. It is interesting to note that the wear debris accumulated at both ends of the wear track. This is quite similar to the wear particle accumulation behavior of macro-scale wear tests (Hwang et al., 1999). The degree of burr formation at the side of the wear track was significantly increased after 70 cycles compared with the 50 cycles sliding case. The 2D profile of the cross-section of the wear track was observed to compare the quantitative degree of wear with respect to the sliding cycle and the normal load. The results are given in Fig. 8. In the case of the 0.5μN normal load, the depth of wear was slightly higher than the roughness level and therefore, it was not easy to obtain the quantitative wear depth. In order to compare these wear depths more clearly, all the 2D profiles of cross-sections of the wear track were averaged. Since the height of the asperities around the wear tack was averaged out, the wear depth at the sub nm level could be obtained. This averaging method could be effectively utilized for the quantification of the nano-wear in the case of the flat specimen. With the increase in the sliding distance and normal load, the wear depth also increased as expected. Under 0.5~1μN normal load, only the deforma-

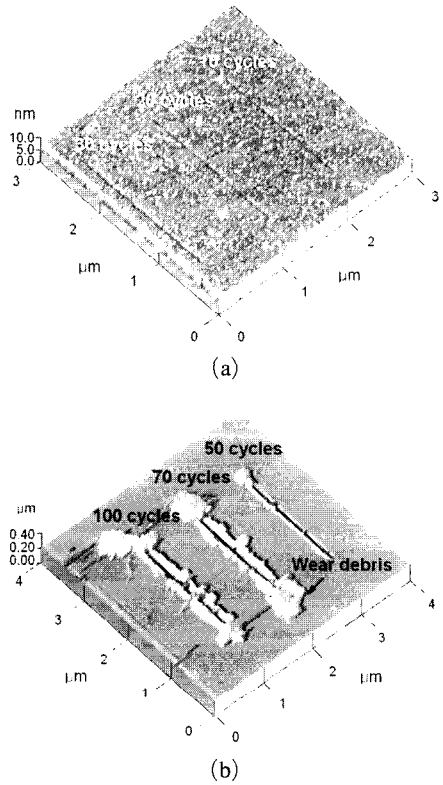

Fig. 7 3D AFM image of the wear track (a) after 10~30 cycles of sliding under 0.5μN normal load and (b) after 50~100 cycles of sliding under 4μN normal load

tion was observed and the wear particles were not significantly generated even after 100 cycle of sliding. However, from Fig. 8 (c), it could be found that the burr at the side of the wear track began to form considerably under 2μN normal load. Also, in the case of the 4μN normal load, large amount of wear debris was formed at the side of the wear track as could be seen in Fig. 8 (d). It is worth noting that the volume of the wear debris was much larger than the wear volume at the track after 70 and 100 cycles of sliding. Therefore, it could be concluded that the significant failure of the amorphous carbon film used in this work occurred between 50 and 70 cycles of sliding under 4μN.

Figure 9 shows the wear rate of the carbon film under various loads. It was found that the wear rate of the carbon film ranged between 4.4×10^{-9} and 1.7×10^{-8}mm^3/N cycle under 0.5~2μN normal load. Even though the wear rate was normalized by the normal load, the wear rate increased with the increase in the normal load which in turn caused an increase in the contact pressure.

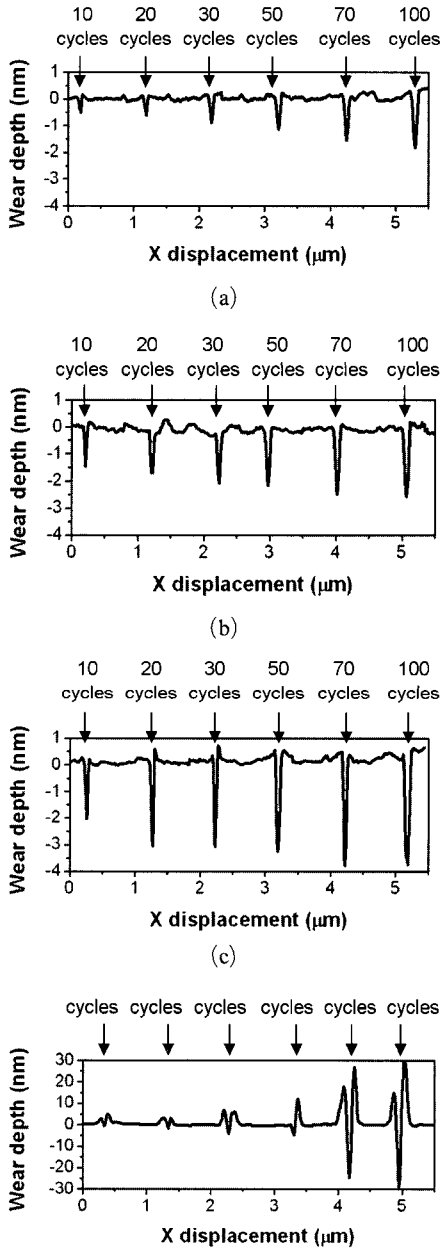

Fig. 8 Averaged 2D AFM image of the wear track after 10~100 cycles of sliding under (a) 0.5, (b) 1.0, (c) 2.0, and (d) 4.0μN normal load

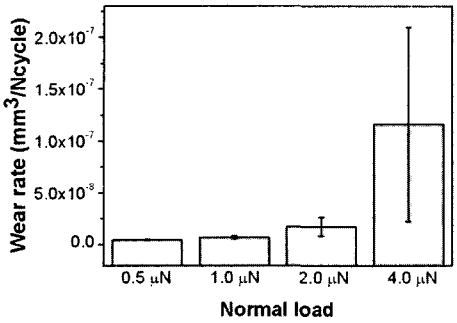

Fig. 9 Wear rate of the carbon film on silicon substrate with respect to the normal load

The wear rate increased to be in the order of 10^{-7} mm^3/N cycle under 4μN normal load after the complete failure of the coated film and the occurrence of the silicon substrate wear.

6. Conclusions

In this work, indentation, ramp-load, and wear tests at the nano-scale were performed based on an AFM. It was shown that the mechanical as well as the tribological characterization of the coated films as thin as a few nm can be attained quantitatively by using these tests. The feasibility of the AFM-based nano-indentation was demonstrated and this method can be effectively utilized if more data and analysis are accumulated. By using the ramp load scratch test using an AFM, the failure of the coated film and the adhesion between the coated film and the substrate could be evaluated. The results showed that the critical load which induced the failure of the carbon film used in this work was about 18μN. Also, from the results of the wear tests, the quantitative wear rate of the ultra-thin carbon film was obtained and the value was in the order of $10^{-9}\sim10^{-8}mm^3/N$ cycle. The approach and test methods used in this work can be effectively utilized for assessment of the mechanical as well as the tribological characteristics of ultra-thin films in the nm regime.

Acknowledgement

This work was supported by the Korea Research Foundation Grant (KRF-2001-041-E00056).

References

Angus, J. C. and Hayman, C. C., 1988, "Low Pressure Metastable Growth of Diamond and Diamond Like Phase," *Science*, Vol. 241, pp. 913~921.

Bellido-Gonzalez, V., Stefanopoulos, N., and Deguilhen, F., 1995, "Friction Monitored Scratch Adhesion Testing," *Surface and Coatings Technology*, Vol. 74~75, pp. 884~889.

Bogdanovic, G., Meurk, A., and Rutland, M. W., 2000, "Tip Friction-Torsional Spring Constant Determination," *Colloids and Surfaces B*, Vol. 19, pp. 397~405.

Bhushan, B. and Koinkar, V. N., 1994, "Nanoindentation Hardness Measurements using Atomic Force Microscopy," *Applied Physics Letters*, Vol. 64, pp. 1653~1655.

Bhushan, B. (Editor), 1998, *Tribology Issues and Opportunities in MEMS*, Kluwer Academic Publisher.

Bhushan, B., 1999a, "Chemical, Mechanical and Tribological Characterization of Ultra-Thin and Hard Amorphous Carbon Coatings as Thin as 3.5nm : Recent Developments," *Diamond and Related Materials*, Vol. 8, pp. 1985~2015.

Bhushan, B., 1999b, *Handbook of Micro/Nanotribology*, CRC press.

Bull, S. J., 1997, "Failure Mode Maps in the Thin Film Scratch Adhesion Test," *Tribology International*, Vol. 30, pp. 491~498.

Chung, K. H. and Kim, D. E., 2003, "Fundamental Investigation of Micro Wear Rate Using an Atomic Force Microscope," *Tribology Letters*, Vol. 15, pp. 135~143.

Erdemir, A., Fenske, G. R., Terry, J., and Wilbur, P., 1997, "Effect of Source Gas and Deposition Method on Friction and Wear Performance of Diamondlike Carbon Films," *Surface and coatings Technology*, Vol. 94-95, pp. 525~530.

Huang, L.-Y., Xu, K.-W., and Li, J., 2002, "Evaluation of Scratch Resistance of Diamond-Like Carbon Films on Ti Alloy Substrate by Nano-Scratch Technique, " *Diamond and Related Materials*, Vol. 11, pp. 1505~1510.

Hwang, D. H., Kim, D. E., and Lee, S. J., 1999,

"Influence of Wear Particle Interaction in the Sliding Interface on Friction of Metals," *Wear*, Vol. 225~229, pp. 427~439.

Khurshudov, A. and Kato, K., 1995, "Wear at the Atomic Force Microscope Tip Under Light Load, Studied by Atomic Force Microscopy," *Ultramicroscopy*, Vol. 60, pp. 11~16.

Krache, B. and Damaschke, B., 2000, "Measurement of Nanohardness and Nanoelasticity of Thin Gold Films with Scanning Force Microscope," *Applied Physics Letters*, Vol. 77, pp. 361~363.

Lemoine, P. and Laughlin, J. Mc, 1999, "Nanomechanical Measurements on Polymer Using Contact Mode Atomic Force Microscopy," *Thin Solid Films*, Vol. 339, pp. 258~264.

Liu, Y., Erdemir, A., and Meletis, E. I., 1996, "A Study of the Wear Mechanism of Diamond-Like Carbon Films," *Surface and Coatings Technology*, Vol, 82, pp. 48~56.

Martinez, E., Andujar, J. L., Polo, M. C., Esteve, J., Robertson, J., and Milne, W. I., 2001, "Study of the Mechanical Properties of Tetrahedral Amorphous carbon Films by Naninden-tation and Nanowear Measurements," *Diamond and Related Materials*, Vol. 10, pp. 145~152.

Menon, A. K., 2000, "Interface tribology for 100 Gb/in^2," *Tribology International*, Vol. 33, pp. 299~308.

Oliver, W. C. and Pharr, G. M., 1992, "An Improved Technique for Determining Hardness and Elastic Modulus Using Load and Displacement Sensing Indentation Experiments," *Journal of Materials Research*, Vol. 7, pp. 1564~1583.

Petzold, M., Landgraf, J., Futing, M., and Olaf, J. M., 1995, "Application of Atomic Force Micro-indentation Testing," *Thin Solid Films*, Vol. 264, pp. 153~158.

Robertson, J, 1992, "Mechanical Properties and Structure of Diamond-Like Carbon," *Diamond and Related Materials*, Vol. 1, pp. 397~406.

Staedler, T. and Schiffman, K., 2001, "Correlation of Nanomechanical and Nanotribological Behavior of Thin DLC Coatings on Different Substrates," *Surface Science*, Vol. 482~485, pp. 1125~1129.

Sundararajan, S. and Bhushan, B., 1998, "Micro/Nanotribological Studies of Polysilicon and SiC Films for MEMS Applications," *Wear*, Vol. 217, pp. 251-261.

Sung, I. H. and Kim, D. E., 2003, "Fabrication of Micro/Nano-Patterns Using MC-SPL (Mechano-Chemical Scanning Probe Lithography) Process," *International Journal of Korean Society of Precision Engineering*, Vol. 4, pp. 22~26.

Valli, J., Maekela, U., Matthews, A., and Murawa, V., 1985, "TiN Coating Adhesion Studies Using the Scratch Test Method," *Journal of Vacuum Science and Technology A*, Vol. 3, pp. 2411~2414.

Zhao, Q., Zhao, Z., Kazazic, E., Embree, M., Trinh, P., Lam, T., and Chang, S., 2002, "Investigation of Scratch Resistance of Thin Carbon Overcoat Media Using Micro Scratch Testing," *Wear*, Vol. 252, pp. 654~661.